INTERFACE MIXED MODE MODEL

R. Walter, J. F. Olesen and H. Stang
Department of Civil Engineering, Technical University of Denmark, Kgs. Lyngby, Denmark

ABSTRACT
A mixed mode model, based on fracture mechanics is presented. The model takes into account gradual softening of shear and normal stresses for normal and sliding crack propagation. The model is introduced and implemented in a commercial finite element package using user-supplied subroutines. Finally, an example using the model is illustrated on debonding of a cement-based overlay bonded to a steel plate.

1 INTRODUCTION

The present study has its origin in an ongoing research project concerned with the strengthening of steel bridge decks using a cement-based overlay [1]. An interface mixed mode model is presented and applied to study the debonding mechanism between a cement-based overlay and a steel plate. A debonding process is often considered a discrete process and modelled as taking place at the bi-material interface. An appropriate model should take into account softening behaviour and the mixed mode nature of the problem involving both shear and normal stresses at the interface.
Much work has been done in the field of softening models for quasi-brittle materials and the present model has its origin in the fictitious model, FCM, by Hillerborg [2]. His concept of a tension softening stress-crack opening relationship in concrete has reached vast acceptance. Less work has been carried out on constitutive modelling of concrete under mixed mode loading. Since the most severe load case for many interfaces is mode 1 loading, emphasis has consequently been placed on making a material description for this case. In the following analysis emphasis is put on opening of an interface in a combined opening mode of shear and tension. The present work is carried out in the framework of Wernersson [3].

2 MODEL

Consider two stress-crack opening relationships: $\tau(\delta_t)$ and $\sigma(\delta_n)$, cf. Figure 1. The curves are described in two parts: The first ascending part is from zero stress to peak stress and is characterized by a very large stiffness, D_t and D_n, to model initial continuous geometry of the interfacial zone. The post peak behaviour is described by a descending, softening part, which relates the stress acting across the crack to the normal opening (δ_n) or sliding (δ_t).

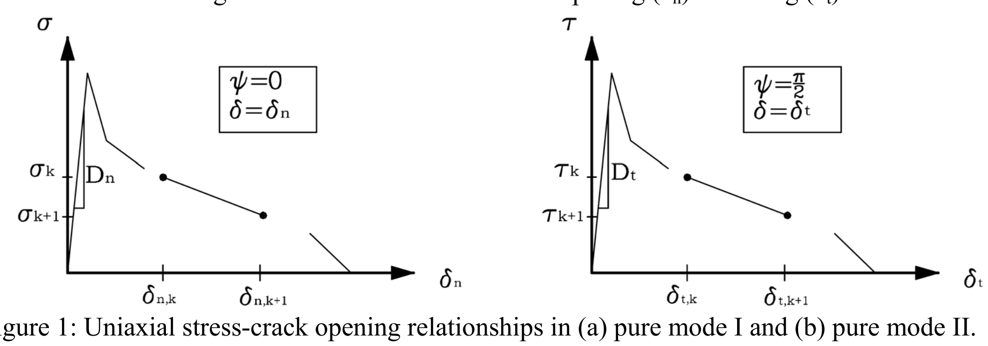

Figure 1: Uniaxial stress-crack opening relationships in (a) pure mode I and (b) pure mode II. The curves are described by a stiff, linear, ascending part until peak stress and a multi linear post peak softening part.

Every linear segment of the complete stress-crack deformation relationship is treated individually. The indices (k) and (k+1) denote the beginning and end of a linear segment. The uniaxial curves are expanded in the (δ_n- δ_t)-plane, so that the normal- and shear stress depends not only on their corresponding displacement, but also on both the shear and normal opening, according to equations (1)-(2).

$$\sigma(\delta_n, \delta_t) \tag{1}$$

$$\tau(\delta_n, \delta_t) \tag{2}$$

In order to describe how the stresses depend on the relative displacements δ_t and δ_n, it is convenient to introduce a polar coordinate system. The mixed mode angle ψ and displacement δ is given by

$$\psi = \arctan\left(\frac{\delta_t}{\delta_n}\right) \tag{3}$$

$$\delta = \sqrt{\delta_n^2 + \delta_t^2} \tag{4}$$

From (3) and (4) δ_t and δ_n may be expressed in terms of δ and ψ, allowing (1) and (2) to be expressed in terms of

$$\sigma(\delta, \psi) \tag{5}$$

$$\tau(\delta, \psi) \tag{6}$$

A failure in pure opening mode (mode I) corresponds to $\delta_t=0 \Rightarrow \psi=0°$ and pure shear cracking (mode II) corresponds to $\delta_n=0 \Rightarrow \psi=90°$. The normal stress-crack opening and shear stress-crack sliding curves maintain their stepwise linear shape for constant ψ, but vary smoothly with the angle ψ. Accordingly, for increasing value of ψ, the normal stress-crack opening curve will diminish from a maximum at $\psi=0°$, while the shear stress crack-sliding curve will expand towards a maximum for $\psi=90°$.

Let δ_k be a δ-value, coupling opening and sliding deformations as in equation (4), describing a kink point on the stress-crack relationship, as shown in Figure 1. The δ_k is linked to opening and sliding deformations by $\delta_{nk,a=}$ $\delta_k \cos\psi$ and $\delta_{sk,a=}$ $\delta_k \sin\psi$ respectively. Index 'k' denotes a kink point on the stress-crack relationship and index 'a' denotes the actual deformation. A criterion, which defines, in coupled terms, the beginning or end of a linear relation, is defined by

$$\left(\frac{\delta_k \cos\psi}{\delta_{n,k}}\right)^m + \left(\frac{\delta_k \sin\psi}{\delta_{t,k}}\right)^n = 1.0 \tag{7}$$

The function in equation (7) is plotted in the δ_n-δ_t plane for the values of the coefficients n and m, (m,n)=(1,1) and (m,n)=(2,2), cf. Figure 2.

In order to define a proper function for δ_k, the function $\delta_k(\psi)$ is introduced for the case where m=n:

$$\delta_k(\psi) = \left[\left(\frac{\cos\psi}{\delta_{n,k}}\right)^m + \left(\frac{\sin\psi}{\delta_{t,k}}\right)^m\right]^{-\frac{1}{m}} \tag{8}$$

The function $\delta_k(\psi)$ is solved for two cases, m being 1 and 2.

$$\delta_k(\psi) = \frac{\delta_{t,k}}{ck\cos\psi + \sin\psi} \quad for \quad m = n = 1 \tag{9}$$

$$\delta_k(\psi) = \frac{\delta_{t,k}}{\sqrt{ck^2\cos^2\psi + \sin^2\psi}} \quad for \quad m = n = 2 \tag{10}$$

where

$$ck = \frac{\delta_{t,k}}{\delta_{n,k}} \tag{11}$$

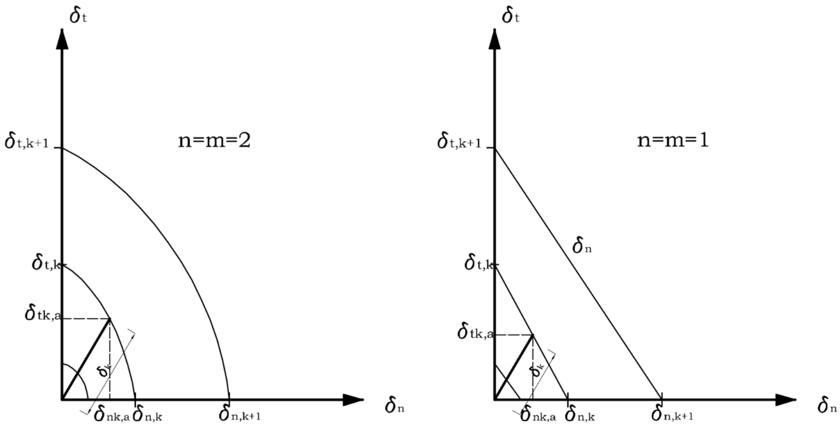

Figure 2: Polar coordinate description. The displacement δ_k for a given mixed mode angle ψ is related to an intersection on the linear softening branch, $\delta_{t,k}$ and $\delta_{n,k}$

Since the stresses change as a function of the mixed mode angle, a breakpoint on the radial stress-crack deformation curve, σ and τ is defined by:

$$\sigma_{k,a} = \frac{ck}{ck + \tan\psi}\sigma_k \tag{12}$$

$$\tau_{k,a} = \frac{\tan\psi}{ck + \tan\psi}\tau_k \tag{13}$$

where the index ‘a’ denotes that the stress is on a radial path. It is easily seen from equations (12) and (13) that

$$\sigma_{k,a} = \begin{cases} \sigma_k & for \quad \psi = 0 \\ 0 & for \quad \psi = \pi/2 \end{cases}$$

$$\tau_{k,a} = \begin{cases} 0 & for \quad \psi = 0 \\ \tau_k & for \quad \psi = \pi/2 \end{cases}$$

For a given value of δ and the angle ψ, the present stresses σ_a and τ_a, somewhere on the line between the two end point (k) and (k+1), can be determined by the two relations

$$\sigma_a = \sigma_{k,a} + \frac{\sigma_{k+1,a} - \sigma_{k,a}}{\delta_{k+1} - \delta_k}\left(\delta - \delta_k\right) \tag{14}$$

$$\tau_a = \tau_{k,a} + \frac{\tau_{k+1,a} - \tau_{k,a}}{\delta_{k+1} - \delta_k}\left(\delta - \delta_k\right) \tag{15}$$

The interface response can be visualized in terms of a stress surface in displacement space e.g. σ_n versus the normal opening and the shear slip. In Figure 3 an example is shown of the coupling effect between normal and shear stresses. The two plots show the variation of normal and shear stresses with respect to the normal and tangential displacements, respectively.

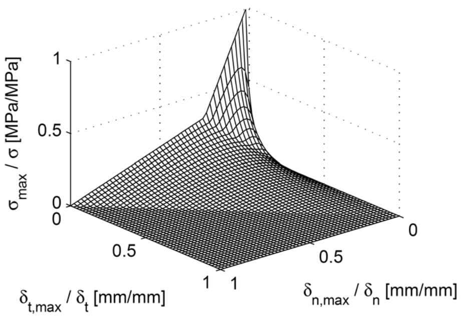

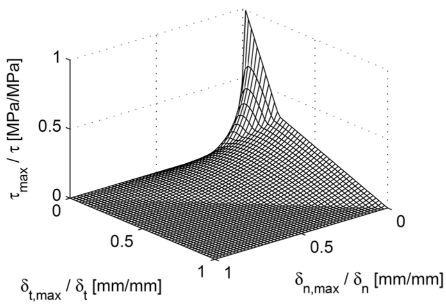

Figure 3: Model visualization, for the case m=n=1 using a uniaxial bilinear softening relations in pure mode I and II. (a) Variation of the normal stress σ with respect to the normal and tangential displacements across the crack. (b) Variation of the shear stress τ with respect to the normal and tangential displacements across the crack.

3 FINITE ELEMENT IMPLEMENTATION AND SIMULATION

The mixed mode model is implemented in a commercial finite element software program, DIANA using user-supplied subroutines. An interface thickness of zero is applied, assuming that the two materials are fully connected prior to cracking. So in the elastic phase, prior interfacial cracking, the initial slopes D_n and D_t are assigned large stiffness values to model continuous geometry. In the finite element analysis, the stiffness components D_{ij} are required, and the stiffness matrix is written as

$$\begin{bmatrix} D_{11} & D_{12} \\ D_{21} & D_{22} \end{bmatrix} = \begin{bmatrix} \dfrac{\partial\sigma}{\partial\delta_n} & \dfrac{\partial\sigma}{\partial\delta_t} \\ \dfrac{\partial\tau}{\partial\delta_n} & \dfrac{\partial\tau}{\partial\delta_t} \end{bmatrix} \tag{16}$$

The matrix can be obtained through standard derivations, preferable with some symbolic mathematical software such as Matlab® or Maple®. A basic assumption for the model is that the deformation δ will be increasing during the loading process. In case of unloading all deformations are supposed to be recoverable, i.e. at negative deformation increments the stress level will follow the same curve as for the case of loading. This is a violation of the expected physical behaviour, thus a limitation of the present model.

A composite beam is studied using the interface mixed mode model. The beam consist of a cement-based overlay bonded to a steel plate, cf. Figure 4. Initially, a stress free, vertical crack in the concrete overlay is present at midspan which causes debonding between the steel and overlay as the beam is loaded.

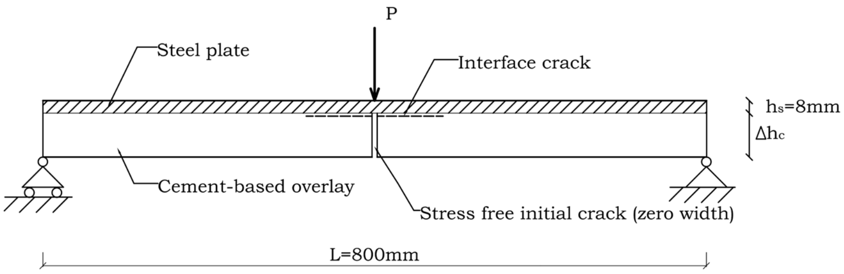

Figure 4: Composite beam (upside down), consisting of a cement-based overlay bonded to a steel plate. The beam has an initial stress free crack and is studied for various heights Δh_c.

The model is applied to the interface between the steel plate and the cement-based overlay. The interface is modelled using standard interface elements available in the applied FEM-package. The interface data needed are the responses in pure mode I and II. In the present simulation, these are defined as: The initial slopes D_t=D_n=1.0e-12, the fracture energy in pure mode I and II is chosen to be 70 and 230 N/m, the maximum normal stress and shear stress are 3.0 and 5.0 MPa respectively, the softening curves are of bilinear type and consist of two points in addition to the ones at crack initiation and are defined by (0.67MPa;0.0026mm) and (0.0MPa;0.1mm) in pure mode I and (1.4MPa;0.05mm) and (0.0MPa;0.15mm) in pure mode II, furthermore, n=m=2.
The cement-based overlay and steel plate are represented by 8-node isoparametric plane stress elements or triangular for mesh refining, cf. Figure 5 for the applied mesh.

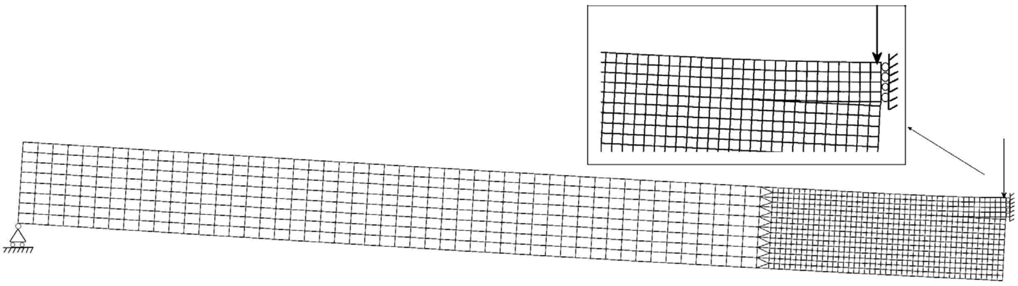

Figure 5: Finite element mesh used in numerical simulations. Only half of the composite beam is modelled.

The model is studied in four simulations for different overlay thicknesses, Δh_c=10, 15, 25 and 50mm. Results are shown in Figure 6 (a)-(b). The mixed mode angle is plotted versus the crack tip propagation measured from the symmetry line. The mixed mode angle, as defined in equation (3), is measured at the peak of normal stress in the fracture process zone. It is seen that for a decreasing overlay thickness, the interface crack mode II contribution increases.
The fracture energy consumed during crack propagation can be obtained from:

$$G_f = \int_{\Gamma} \left(\sigma d\delta_n + \tau d\delta_s \right) \tag{17}$$

Where Γ is the deformation path that results in complete separation of the interface, thus the total fracture energy is path dependent in the present analysis. The energy consumption is plotted versus the overlay thickness, cf. Figure (6b). It is seen that for decreasing thickness, mode II energy and total fracture energy consumed are both increased. The different fracture energy contributions are calculated for a fully separated, stress free crack, of 100mm measured from the symmetry line of the composite beam.

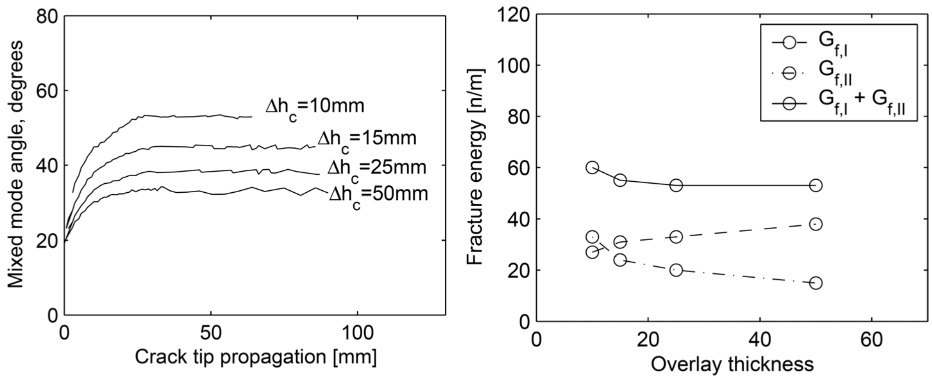

Figure 6: (a) Mixed mode angle ψ versus crack tip position for different overlay thicknesses. (b) Energy consumption for different overlay thicknesses at the propagation of a fully separated crack of 100mm from the symmetry line.

4 CONCLUSIONS

An interfacial mixed mode model has been presented and implemented into a commercial finite element program as a constitutive interface model. The model has been used to study the debonding behaviour on a composite beam with various overlay thicknesses. It is seen from the numerical simulation, that for a decreasing overlay thickness, the interfacial crack is more likely to propagate in mode II, which could very well be the explanation for the better bond of thin overlays generally observed in practice.

5 REFERENCES

[1] Walter, R., Gimsing N-J. and Stang, H., Composite Steel-Concrete orthotropic Bridge Deck, In the proceedings of the Nordic Steel Conference – NSCC2004, Copenhagen, Denmark, 7-9 June, 2004.

[2] Hillerborg, A., Modéer, M. and Petersson, P. Analysis of crack formation and crack growth in concrete by means of fracture mechanics and finite elements. Cem. Concre. Res., 6(6):773-782, 1976.

[3] Wernersson, H. Fracture characterization of wood adhesive joints. Report TVSM-1006, Lund University, Division of Structural Mechanics, 1994.